Development of a Generalized Framework for Point and Lidar Measurement Sensitivities in Turbulent, Complex Flow

Andrew H. Black, Jean-Pierre Cariou, Frédéric Delbos

24 May 2023

VAISALA

Motivation

Turbulence influences wind measurements of both 1st and 2nd moments, introducing both systematic biases and increased uncertainties to anemometers and lidars (Clive, 2008; Newman, 2015; Rosenbusch, 2021)

These biases can be quantified and corrected, and described empirically as uncertainties via device Classification following IEC 61400-50-1, -50-2, -50-3, -50-4, or other demonstrations of uncertainty and bias in measurements

Device Classifications can be limited to certain turbulence or flow complexity domains

A general framework for understanding turbulence sensitivities for all device types would enable better understanding of device performance in conditions outside the empirical Classification performance envelope, and enable more refined comparisons between different sensors, especially for new applications

In this presentation, we propose such a generalized framework and show preliminary results for lidar in complex terrain

Wind Measurement Geometry

- All sensors sample the wind with a collection of “probes” of varying orientation

Cup anemometer

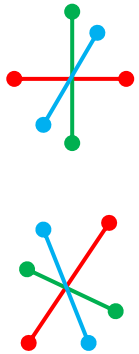

Ultrasonic anemometer

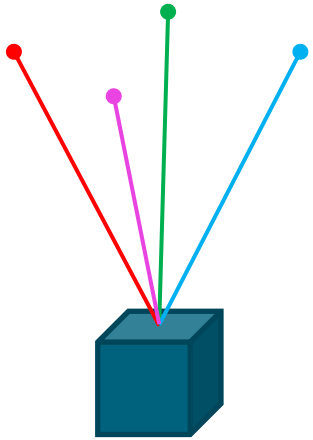

Profiling lidar

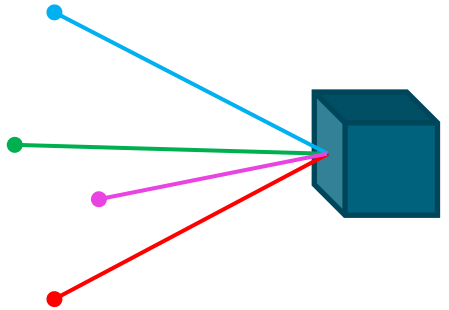

Nacelle-mounted lidar

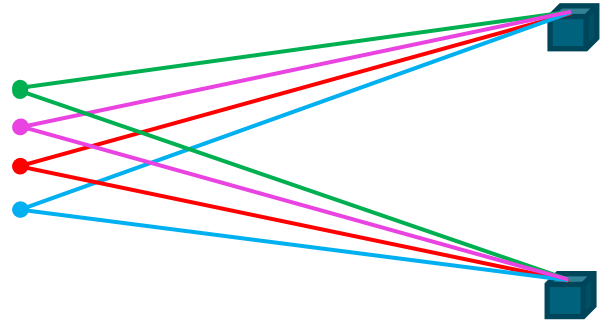

Dual scanning lidar

- These orientations can all be described using *SO(3) rotation group*

$$R_x(\theta_x) = \begin{bmatrix} 1 & 0 & 0 \\ 0 & \cos\theta_x & -\sin\theta_x \\ 0 & \sin\theta_x & \cos\theta_x \end{bmatrix}, \; R_y(\theta_y) = \begin{bmatrix} \cos\theta_y & 0 & \sin\theta_y \\ 0 & 1 & 0 \\ -\sin\theta_y & 0 & \cos\theta_y \end{bmatrix}, \; R_z(\theta_z) = \begin{bmatrix} \cos\theta_z & -\sin\theta_z & 0 \\ \sin\theta_z & \cos\theta_z & 0 \\ 0 & 0 & 1 \end{bmatrix}.$$

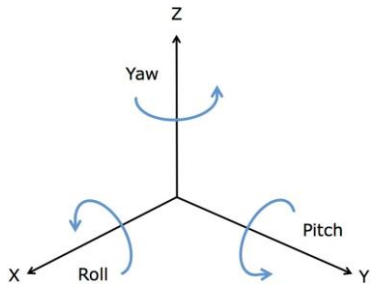

Wind Flow Geometry

- Wind vector orientations vary depending on terrain and turbine flow interactions

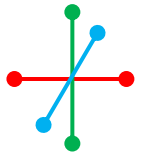

Simple flow

Tilted flow

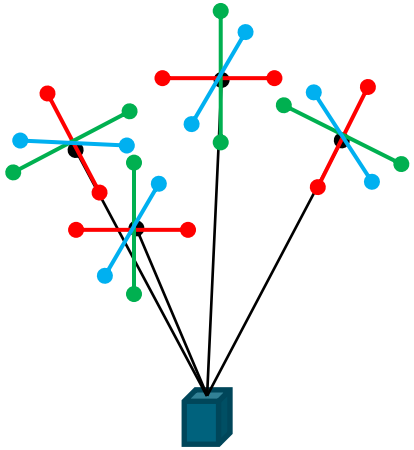

Complex flow, Profiling lidar

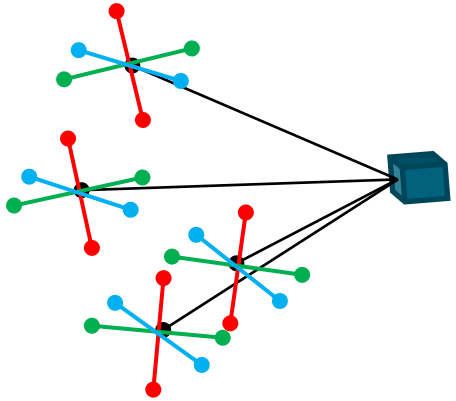

Induction zone, nacelle-mounted lidar

- Described using *SO(3) rotation group* and *Reynolds decomposition*
- $\begin{bmatrix} \bar{u} + u' \\ \bar{v} + v' \\ w' \end{bmatrix}$ encodes assumptions about boundary layer flow : flat ($\bar{w} = 0$) and turbulent

SO(3) and Reynolds Decomposition

Example: North Beam v_N of a WindCube lidar derived: $R_z(0°)R_y(-62°)\boldsymbol{u} = \begin{bmatrix}\cos(62°)\\0\\\sin(62°)\end{bmatrix}$

Project Reynolds-decomposed wind to beam: $[\cos(62°) \quad 0 \quad \sin(62°)]\begin{bmatrix}\bar{u}+u'\\\bar{v}+v'\\w'\end{bmatrix} = \cos(62°)\,(\bar{u}+u') + \sin(62°)\,w'$

Repeat for all measurement orientations. Take pseudo-inverse to derive A^+

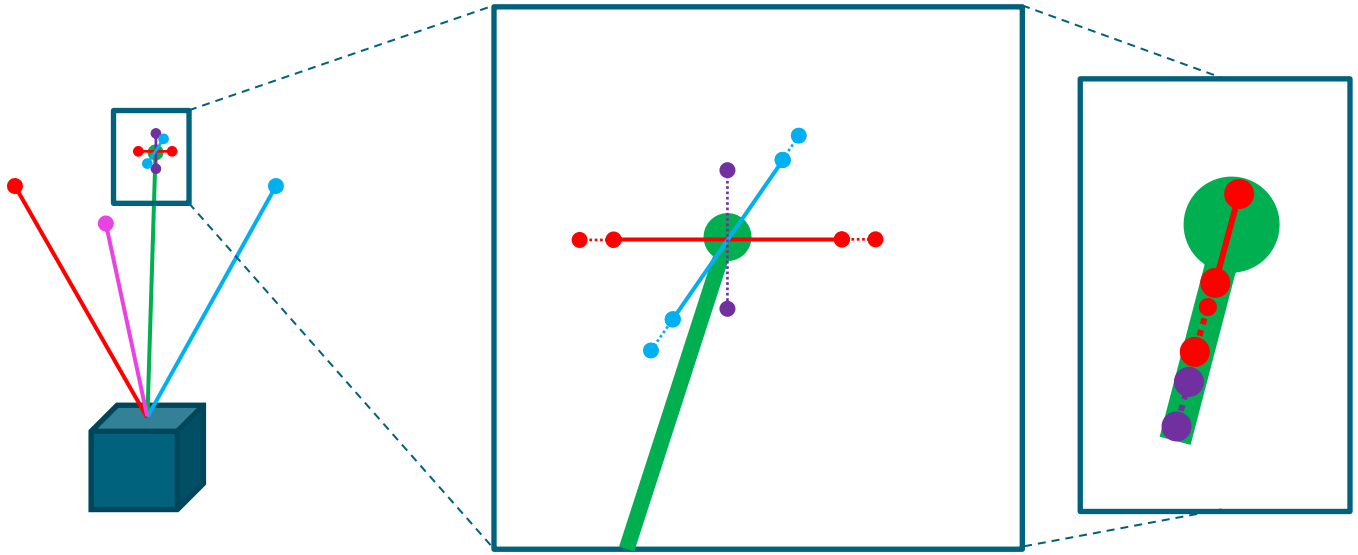

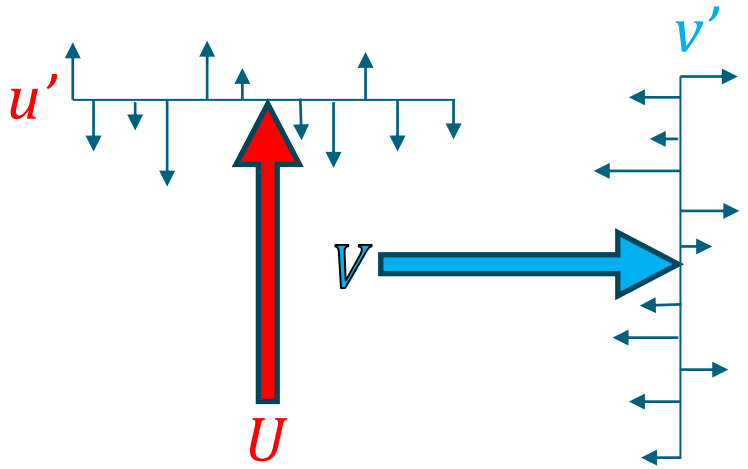

Wind Field Reconstruction

- ℓ_2 norm of the horizontal component of the wind (other statistics exist as well)

Scalar averaging ("reconstruct-then-average")

$$U_{scalar} = \frac{1}{N}\sum_{i=1}^{N} \|PA^{+}v_r\|_{2,i}$$

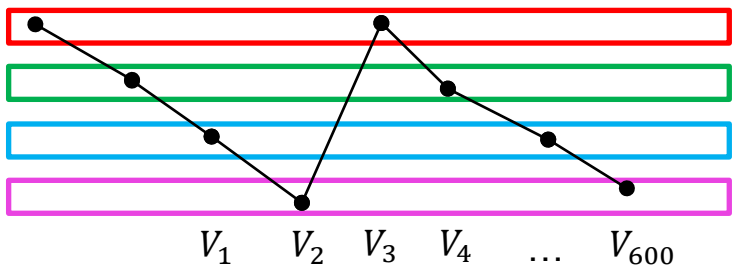

Vector averaging ("average-then-reconstruct")

$$U_{vector} = \|PA^{+}\overline{v_r}\|_2$$

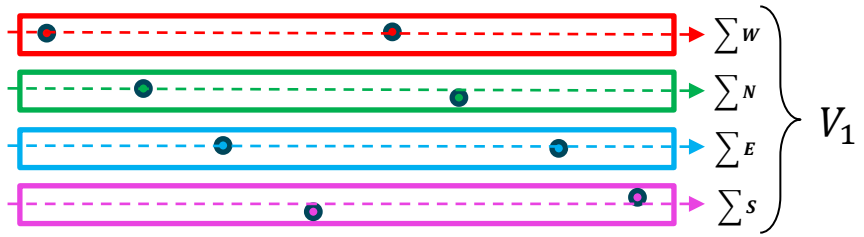

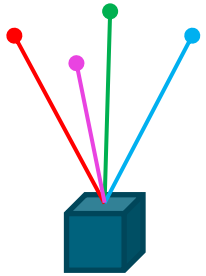

Profiling lidar

- Widely used, well known to have different sensitivities to turbulence
- Averaged together with variable weights in WindCube v2.1 (**Hybrid WFR**)

VAISALA

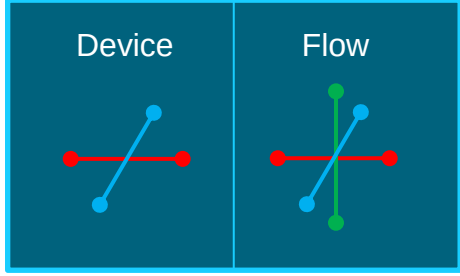

Perturbation Method – Horizontal Wind Speed

Anemometer in flat, turbulent flow

- Rosenbusch (2021) and Robey (2022) use 2nd order Taylor series expansion
- For more complex flows and devices this method is quite cumbersome
- We propose a **perturbation method** to examine these sensitivities:

$$U_{scalar,1Hz} = \sqrt{\boldsymbol{u^2} + \boldsymbol{v^2}} = \sqrt{\bar{u}^2 + 2\bar{u}u' + u'^2 + \bar{v}^2 + 2\bar{v}v' + v'^2}$$

Expand the Reynolds decomposition

$$= \sqrt{\bar{u}^2 + \bar{v}^2}\sqrt{1 + \frac{1}{\bar{u}^2+\bar{v}^2}[2\bar{u}u' + u'^2 + 2\bar{v}v' + v'^2]}$$

Factor out the vector average

2nd term is suitable for **binomial approximation**

$$(1+\epsilon)^\alpha \approx 1 + \alpha\epsilon + \frac{\alpha(\alpha-1)}{2!}\epsilon^2 + \mathcal{O}(3)$$

$$= U_{vector}\left[1 + \frac{1}{2U_{vector}^2}[2\bar{u}u' + u'^2 + 2\bar{v}v' + v'^2] - \frac{1}{8U_{vector}^4}[4\bar{u}^2u'^2 + 4\bar{v}^2v'^2 + 8\bar{u}\bar{v}u'v']\right]$$

* dropping $\mathcal{O}(3)$ terms *

Limit of application:

- $\epsilon \ll 1$
- Likely not applicable for low speeds with high turbulence

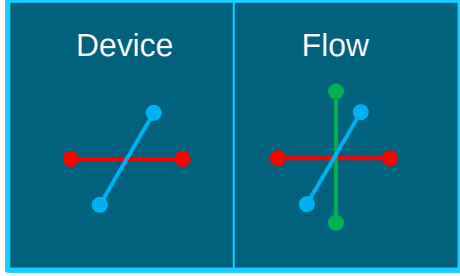

Perturbation Method – Horizontal Wind Speed

Anemometer in flat, turbulent flow

$$U_{scalar,1Hz} = U_{vector}\left[1 + \frac{1}{2U_{vector}^2}\left[2\bar{u}u' + u'^2 + 2\bar{v}v' + v'^2\right] - \frac{1}{8U_{vector}^4}\left[4\bar{u}^2u'^2 + 4\bar{v}^2v'^2 + 8\bar{u}\bar{v}u'v'\right]\right]$$

$$U_{scalar} = U_{vector}\left[\overline{1 + \frac{1}{2U_{vector}^2}\left[u'^2 + v'^2\right] - \frac{1}{2U_{vector}^4}\left[\bar{u}^2u'^2 + \bar{v}^2v'^2 + 2\bar{u}\bar{v}u'v'\right]}\right]$$

apply time averaging, drop linear terms

$$U_{scalar} = U_{vector}\left[\overline{1 + \frac{1}{2U_{vector}^2}\left[u'^2 + v'^2\right] - \frac{1}{2U_{vector}^4}\left[U_{vector}\cdot\overrightarrow{U'}\right]^2}\right]$$

Re-express as square of dot product of mean and turbulent terms

$$U_{scalar} = U_{vector}\left[\overline{1 + \frac{1}{2U_{vector}^2}\left[u'^2 + v'^2\right] - \frac{1}{2U_{vector}^2}\left[u'^2 + v'^2\right]\cos^2\theta}\right]$$

Simplify, θ is the angle between U_{vector} and $\overrightarrow{U'}$

$$U_{scalar} = U_{vector}\left[1 + \frac{1}{2U_{vector}^2}\overline{\left[u'^2 + v'^2\right]\sin^2\theta}\right] = U_{vector} + \frac{1}{2U_{vector}}\overline{\left\|\overrightarrow{U'}\right\|_2^2\sin^2\theta}$$

- This result is identical to the 2nd order Taylor expansion demonstrated in the literature

Conclusion: the Perturbation Method is adequate for this application

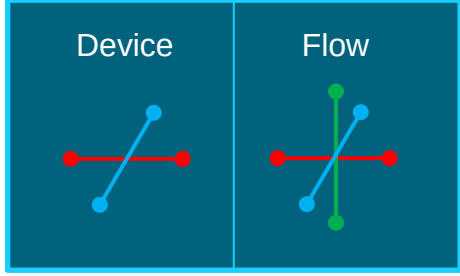

Perturbation Method – Horizontal Wind Speed

Anemometer in flat, turbulent flow

$$U_{scalar} = U_{vector}\left[1 + \frac{1}{2U_{vector}^2}\overline{[u'^2 + v'^2]\sin^2\theta}\right] = U_{vector} + \frac{1}{2U_{vector}}\overline{\left\|\overrightarrow{U'}\right\|_2^2 \sin^2\theta}$$

$$U_{scalar} = U_{vector} + \frac{1}{2U_{vector}}\sum_{i,j=1}^{3}\begin{bmatrix}1 & 0 & 0\\ 0 & 1 & 0\\ 0 & 0 & 0\end{bmatrix} \circ \overline{\begin{bmatrix}\overline{u'^2} & \overline{u'v'} & \overline{u'w'}\\ \overline{v'u'} & \overline{v'^2} & \overline{v'w'}\\ \overline{w'u'} & \overline{w'v'} & \overline{w'^2}\end{bmatrix}\sin^2\theta}$$

- The scalar averaging sensitivity term is the sum of the element-wise product of:
  - Reynolds stress tensor, τ_{ij}
  - Scalar inflation tensor, γ_{ij}
  - Lateral wind direction fluctuation, $\sin^2\theta$
  - Normalized by ½ of the vector average wind speed
- Commonly understood as wind direction variance or transverse fluctuations

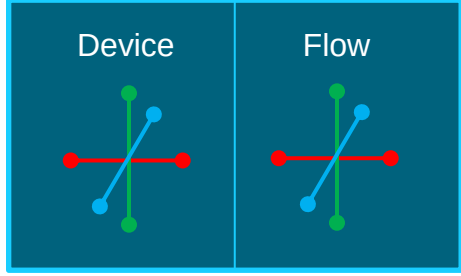

Perturbation Method – 3D Wind Speed

3D Anemometer in flat, turbulent flow

$$U_{scalar} = U_{vector}\left[1 + \frac{1}{2U_{vector}^2}\overline{[u'^2 + v'^2 + w'^2]\sin^2\theta}\right] = U_{vector} + \frac{1}{2U_{vector}}\overline{\left\|\overrightarrow{U'}\right\|_2^2 \sin^2\theta}$$

$$U_{scalar} = U_{vector} + \frac{1}{2U_{vector}}\sum_{i,j=1}^{3}\begin{bmatrix}1 & 0 & 0\\ 0 & 1 & 0\\ 0 & 0 & 1\end{bmatrix} \circ \overline{\begin{bmatrix}\overline{u'^2} & \overline{u'v'} & \overline{u'w'}\\ \overline{v'u'} & \overline{v'^2} & \overline{v'w'}\\ \overline{w'u'} & \overline{w'v'} & \overline{w'^2}\end{bmatrix}\sin^2\theta}$$

- The sensitivity of a 3D scalar measurement is different than 2D
  - w'^2 component is included
  - $\sin^2\theta$ includes fluctuations in 3D
  - Note: $\overline{\sin^2\theta_{2D,iso}} = \frac{1}{2}$, $\overline{\sin^2\theta_{2D,Kaimal}} = 0.41$, $\overline{\sin^2\theta_{3D,iso}} = \frac{2}{3}$, $\overline{\sin^2\theta_{3D,Kaimal}} = 0.53$ (varies as $\overline{u'^2}$:$\overline{v'^2}$:$\overline{w'^2}$)

Question: what is the difference between 2D and 3D vector measurements?

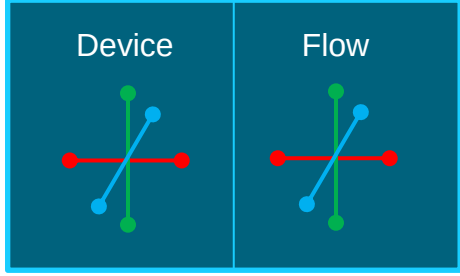

Perturbation Method – 3D Wind Speed

3D Anemometer in flat, turbulent flow

$$U_{scalar} = U_{vector}\left[1 + \frac{1}{2U_{vector}^2}\overline{[u'^2 + v'^2 + w'^2]\sin^2\theta}\right] = U_{vector} + \frac{1}{2U_{vector}}\overline{\left\|\overrightarrow{U'}\right\|_2^2 \sin^2\theta}$$

$$U_{scalar} = U_{vector} + \frac{1}{2U_{vector}}\sum_{i,j=1}^{3}\begin{bmatrix}1 & 0 & 0\\ 0 & 1 & 0\\ 0 & 0 & 1\end{bmatrix} \circ \overline{\begin{bmatrix}\overline{u'^2} & \overline{u'v'} & \overline{u'w'}\\ \overline{v'u'} & \overline{v'^2} & \overline{v'w'}\\ \overline{w'u'} & \overline{w'v'} & \overline{w'^2}\end{bmatrix}\sin^2\theta}$$

To 1st order (only difference: no $\sin^2\theta$), the sensitivity term is:

$$U_{scalar} = U_{vector} + \frac{\frac{1}{2}\left(\overline{u'^2} + \overline{v'^2} + \overline{w'^2}\right)}{U_{vector}}$$

exactly the ratio of the turbulent kinetic energy to the vector average wind speed

To 2nd order, $\sin^2\theta$ reduces the scalar inflation term to the lateral projection of τ_{ij} terms:

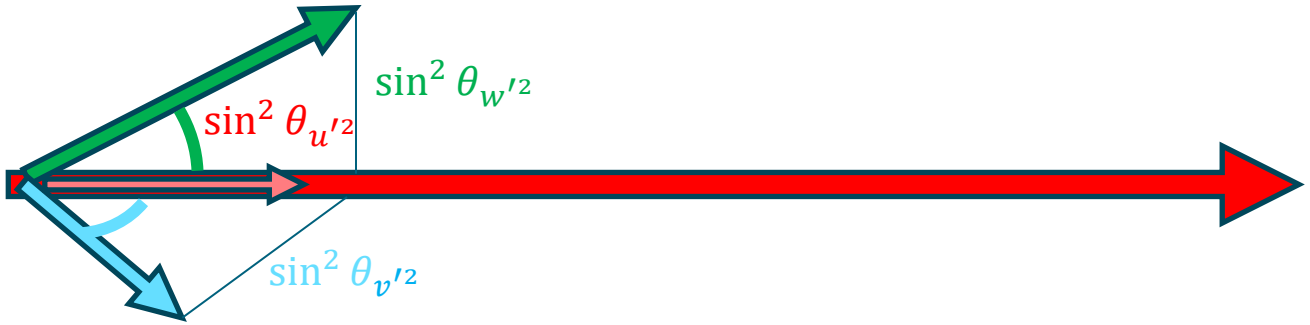

Application to Inclined Flow

VAISALA

Perturbation Method – Horizontal Wind Speed

Anemometer in inclined, turbulent flow

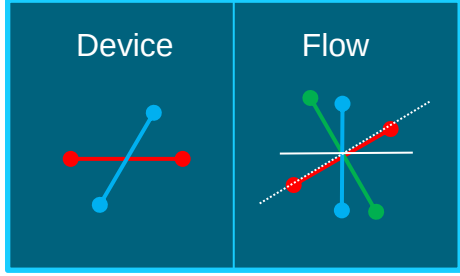

- Introduce arbitrary tilt θ_y to the wind reference frame along the *u*-axis with SO(3) group:

$$\begin{bmatrix} \cos\theta_y & 0 & \sin\theta_y \\ 0 & 1 & 0 \\ -\sin\theta_y & 0 & \sin\theta_y \end{bmatrix} \begin{bmatrix} \bar{u}+u' \\ \bar{v}+v' \\ w' \end{bmatrix} = \begin{bmatrix} \cos\theta_y\,(\bar{u}+u') + \sin\theta_y w' \\ \bar{v}+v' \\ -\sin\theta_y(\bar{u}+u') + \cos\theta_y\, w' \end{bmatrix} = \begin{bmatrix} \cos\theta_y\,\bar{u} \\ \bar{v} \\ -\sin\theta_y\bar{u} \end{bmatrix} + \begin{bmatrix} \cos\theta_y\,u' + \sin\theta_y w' \\ v' \\ -\sin\theta_y u' + w' \end{bmatrix}$$

- Express ℓ_2 norm of ***u-*** and ***v-***components (the device measurements):

$$U_{scalar,1Hz} = \sqrt{\left(\cos\theta_y\,(\bar{u}+u') + \sin\theta_y w'\right)^2 + (\bar{v}+v')^2}$$

- Factor out average terms:

$$U_{scalar,1Hz} = \sqrt{\left(\cos\theta_y\,\bar{u}\right)^2 + \bar{v}^2}\sqrt{1 + \underbrace{\frac{1}{\left(\cos\theta_y\,\bar{u}\right)^2 + \bar{v}^2}\left[2\cos^2\theta_y\,\bar{u}u' + 2\cos\theta_y\sin\theta_y\,\bar{u}w' + \cos^2\theta_y\,u'^2 + 2\cos\theta_y\sin\theta_y\,u'w' + \sin^2\theta_y\,w'^2 + 2\bar{v}v' + v'^2\right]}_{\alpha}}$$

Perturbation Method – Horizontal Wind Speed

Anemometer in inclined, turbulent flow

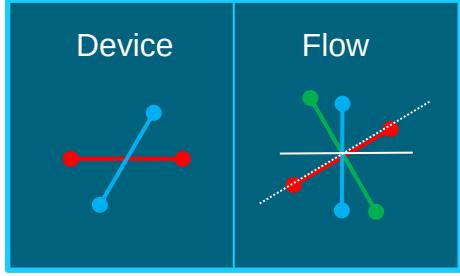

$$U_{scalar,1Hz} = \sqrt{\left(\cos\theta_y\,\bar{u}\right)^2 + \bar{v}^2}\sqrt{1 + \underbrace{\frac{1}{\left(\cos\theta_y\,\bar{u}\right)^2 + \bar{v}^2}\left[2\cos^2\theta_y\,\bar{u}u' + 2\cos\theta_y\sin\theta_y\,\bar{u}w' + \cos^2\theta_y\,u'^2 + 2\cos\theta_y\sin\theta_y\,u'w' + \sin^2\theta_y\,w'^2 + 2\bar{v}v' + v'^2\right]}_{\alpha}}$$

- Apply 2nd order binomial expansion:

$$U_{scalar,1Hz} = U_{vector}\left[1 + \frac{\alpha}{2} - \frac{\alpha^2}{8}\right]$$

- Make a pot of coffee, then expand all 1st and 2nd order terms
- Apply time averaging (eliminates 1st order terms)

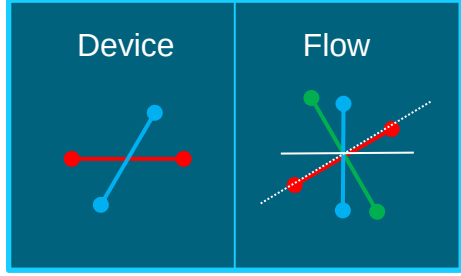

Perturbation Method – Horizontal Wind Speed

Anemometer in inclined, turbulent flow

- Re-express the 2nd order term:

$$U_{scalar,1Hz} = U_{vector}\left[1 + \frac{\cos^2\theta_y\, u'^2 + 2\cos\theta_y \sin\theta_y\, u'w' + \sin^2\theta_y\, w'^2 + v'^2}{2U_{vector}^2} - \frac{4\left[U_{vector}\cdot\overrightarrow{U'}\right]^2}{8U_{vector}^4}\right]$$

where: $\overrightarrow{U'} = \begin{bmatrix}\cos\theta_y\, u' + \sin\theta_y w' \\ v'\end{bmatrix}$ $\quad U_{vector} = \begin{bmatrix}\cos\theta_y\, \bar{u} \\ \bar{v}\end{bmatrix}$

and: $\left\|\overrightarrow{U'}\right\|_2^2 = \cos^2\theta_y\, u'^2 + 2\cos\theta_y \sin\theta_y\, u'w' + \sin^2\theta_y\, w'^2 + v'^2$

Yielding the same form: $U_{vector} + \frac{1}{2U_{vector}}\overline{\left\|\overrightarrow{U'}\right\|_2^2 \sin^2\theta}$

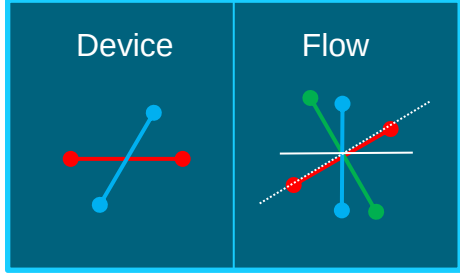

Perturbation Method – Horizontal Wind Speed

Anemometer in inclined, turbulent flow

- Or equivalently:

$$\overline{U}_{scalar} = U_{vector} + \frac{1}{2U_{vector}} \sum_{i,j=1}^{3} \begin{bmatrix} \cos^2\theta_y & 0 & \sin\theta_y \cos\theta_y \\ 0 & 1 & 0 \\ \sin\theta_y \cos\theta_y & 0 & \sin^2\theta_y \end{bmatrix} \circ \overline{\tau_{ij} \sin^2\theta}$$

- We expect $\sqrt{(\cos\theta_y\,\bar{u})^2 + \bar{v}^2}$, the cosine response, but for a scalar average we have a new, sensitivity term depending on:

  $\theta_y, \theta, \overline{u'^2}, \overline{u'w'}, \overline{v'^2}$, and $\overline{w'^2}$
- Covariance between τ_{ij} and direction variation θ enters via time-averaging

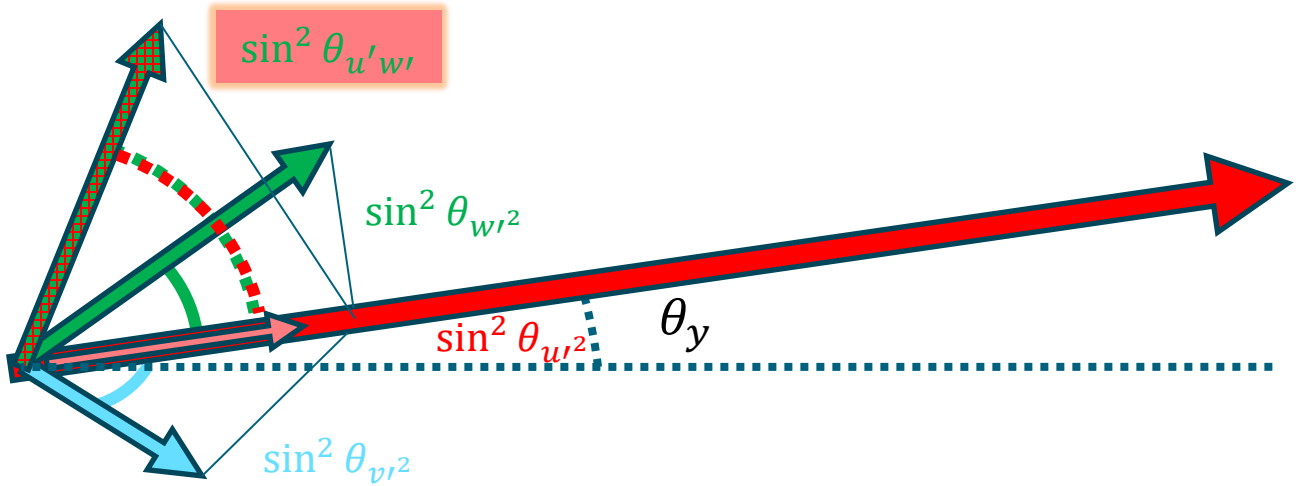

Perturbation Method – Limits of applicability

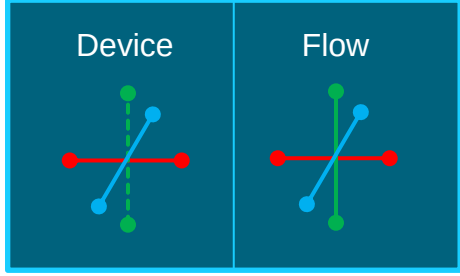

- Comparison between direct scalar averages and $U_{vector} + \frac{1}{2U_{vector}} \overline{\left\| \overrightarrow{U'} \right\|_2^2 \sin^2 \theta}$
- For normal, random *uvw* turbulence
  - u’ = TI * U (set to 6 m/s)
  - v’ = 0.7 u’
  - w’ = 0.5 u’
  - 600 samples per average
  - 100 averages per turbulence level
- Perturbation method predicts scalar sensitivity term within 10% of real value for turbulence intensity values up to ~35%

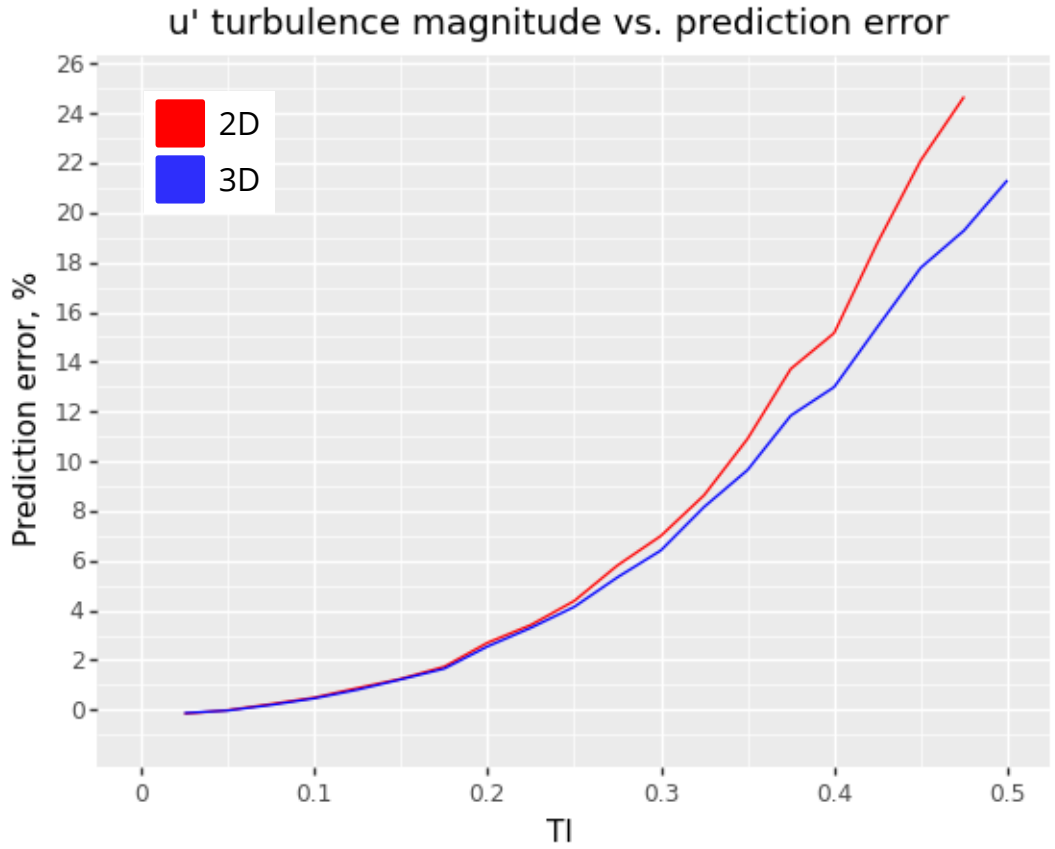

Perturbation Method – Horizontal Wind Speed

Anemometers in complex turbulent flow

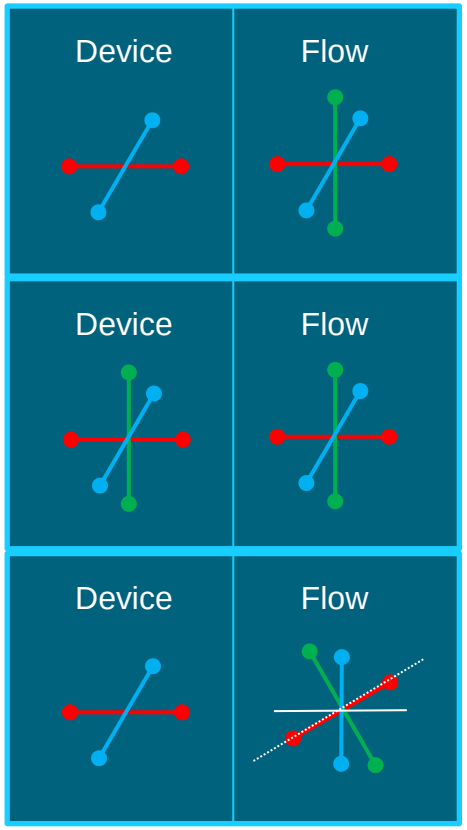

$$\begin{bmatrix} 1 & 0 & 0 \\ 0 & 1 & 0 \\ 0 & 0 & 0 \end{bmatrix}$$

$$\begin{bmatrix} 1 & 0 & 0 \\ 0 & 1 & 0 \\ 0 & 0 & 1 \end{bmatrix}$$

$$\begin{bmatrix} \cos^2\theta_y & 0 & \sin\theta_y \cos\theta_y \\ 0 & 1 & 0 \\ \sin\theta_y \cos\theta_y & 0 & \sin^2\theta_y \end{bmatrix}$$

- *in situ* measurements' turbulence sensitivities can be described compactly using this sensitivity tensor
- The Reynolds stress tensor same for all configurations
- $\overline{\sin^2\theta}$ can be 2D or 3D

Application to Lidar

VAISALA

$d\tau_{ij}$ for Spatially-Separated Lidar Beams

- When combining measurements from different beams, the turbulent components are not exactly equal
- $u'_N - u'_S \neq 0$ and $u'_N + u'_S \neq 2u'$
- **This is a key difference from *in situ* or converging beam configurations**
- One must carefully track $du'_{N\pm}$ terms to properly derive the scalar inflation tensor, γ_{ij}
- Note link to Squeeze WFR: $u'_{N,t0} - u'_{S,t1} = 0$
- Detail in Appendix

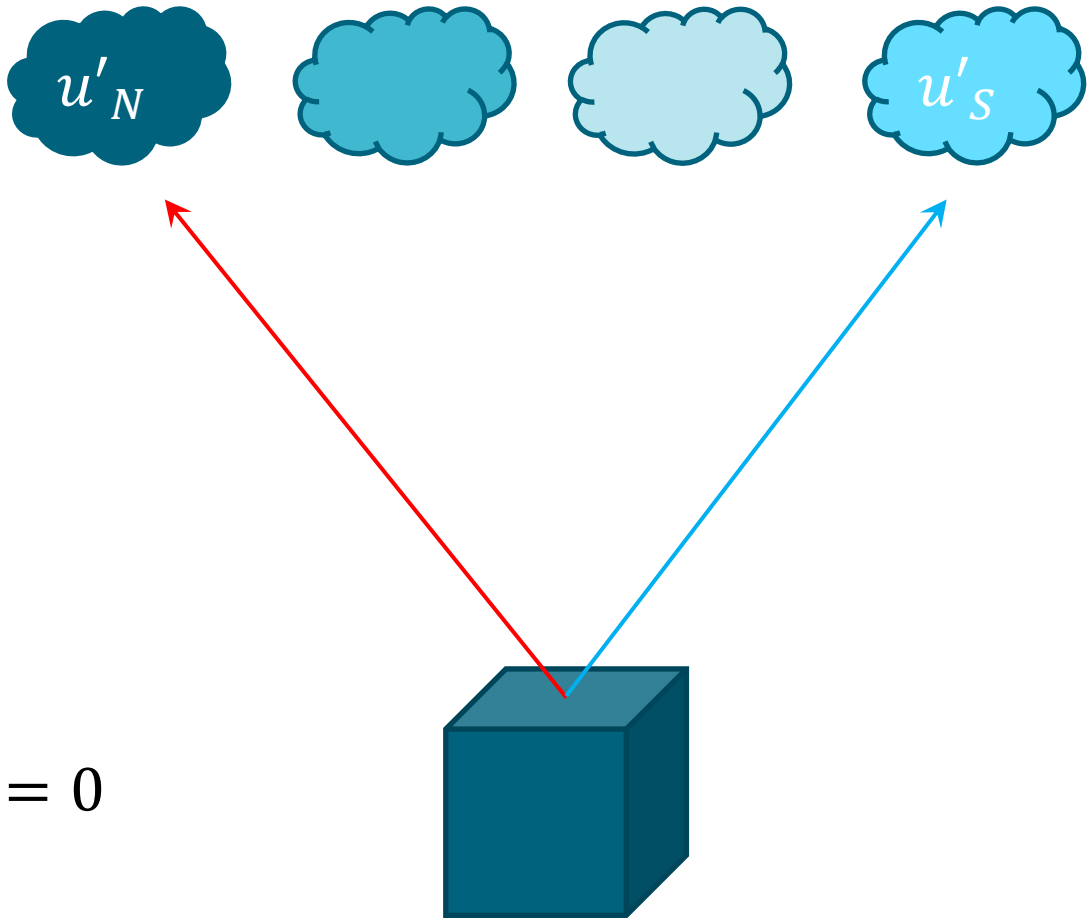

Perturbation Method – Horizontal Wind Speed

Four-beam lidar in various flows

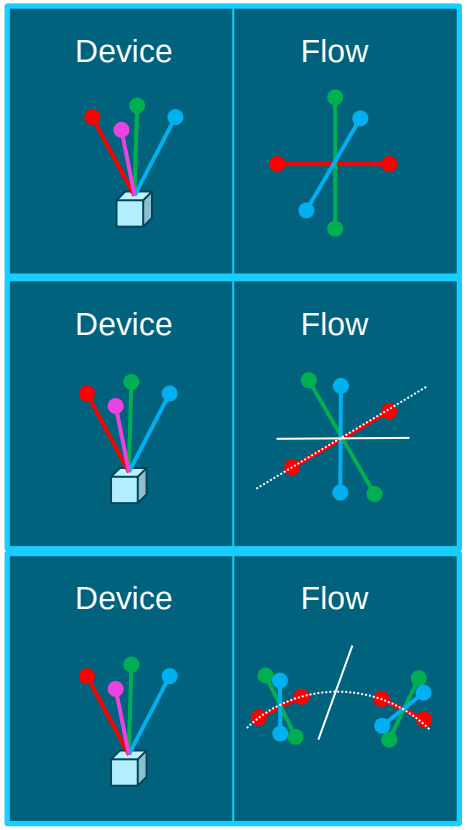

$$\begin{bmatrix} 1 & 0 & \tan\varphi \\ 0 & 1 & \tan\varphi \\ \tan\varphi & \tan\varphi & 2\tan^2\varphi \end{bmatrix}$$

$$\begin{bmatrix} \cos^2\theta_y & \sin\theta_y\tan\varphi & \cos^2\theta_y\tan\varphi \\ \sin\theta_y\tan\varphi & 1 & \cos\theta_y\tan\varphi \\ \cos^2\theta_y\tan\varphi & \cos\theta_y\tan\varphi & 2\cos^2\theta_y\tan^2\varphi \end{bmatrix}$$

$$\begin{bmatrix} \cos^2\theta_y + \sin^2\theta_y\tan^2\varphi & 0 & \frac{1}{2}\sin 2\theta_y\sec^2\varphi + \tan\varphi \\ 0 & 1 & \tan\varphi \\ \frac{1}{2}\sin 2\theta_y\sec^2\varphi + \tan\varphi & \tan\varphi & \sin^2\theta_y + \sin 2\theta_y\tan\varphi + \left(1+\cos^2\theta_y\right)\tan^2\varphi \end{bmatrix}$$

- φ is the lidar beam angle relative to horizontal (62° for a WindCube)
- Perturbation Method validated against $\left\|\overrightarrow{U'}\right\|_2^2$ for simple case
- $\left\|\overrightarrow{U'}\right\|_2^2$ used directly for complex flows
- $d\tau_{ij}$ detail in Appendix

Generalized Framework

$$\bar{U}_{scalar} = U_{vector} + \frac{1}{2U_{vector}} \overline{\left\| \overrightarrow{U'} \right\|_2^2 \sin^2\theta}$$

$$\bar{U}_{scalar} = U_{vector} + \frac{1}{2U_{vector}} \sum_{i,j=1}^{3} \gamma_{ij} \circ \overline{d\tau_{ij} \sin^2\theta}$$

- This formula describes scalar WFR sensitivities to flow inclination, wind orientation fluctuations, and all terms of the Reynolds stress tensor, simultaneously

- Naturally includes covariance between turbulent terms in time averaging
- Derived from first principles
- Equivalence between 2nd order Taylor expansion, 2nd order Perturbation Method, and $\left\| \overrightarrow{U'} \right\|_2^2$
- Can accommodate wide variety of geometries and flows
- Provides a clear toolkit for hybridization and WFR selection for different applications

Lidar in Complex Flow for Wind Resource Assessment

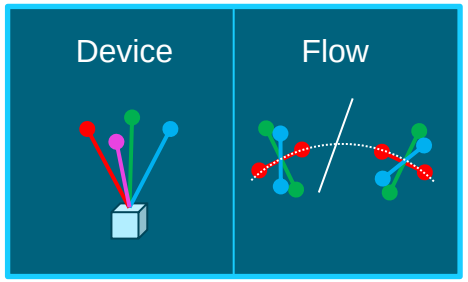

$$\begin{bmatrix} \cos^2\theta_y + \sin^2\theta_y \tan^2\varphi & 0 & \frac{1}{2}\sin 2\theta_y \sec^2\varphi + \tan\varphi \\ 0 & 1 & \tan\varphi \\ \frac{1}{2}\sin 2\theta_y \sec^2\varphi + \tan\varphi & \tan\varphi & \sin^2\theta_y + \sin 2\theta_y \tan\varphi + \left(1+\cos^2\theta_y\right)\tan^2\varphi \end{bmatrix}$$

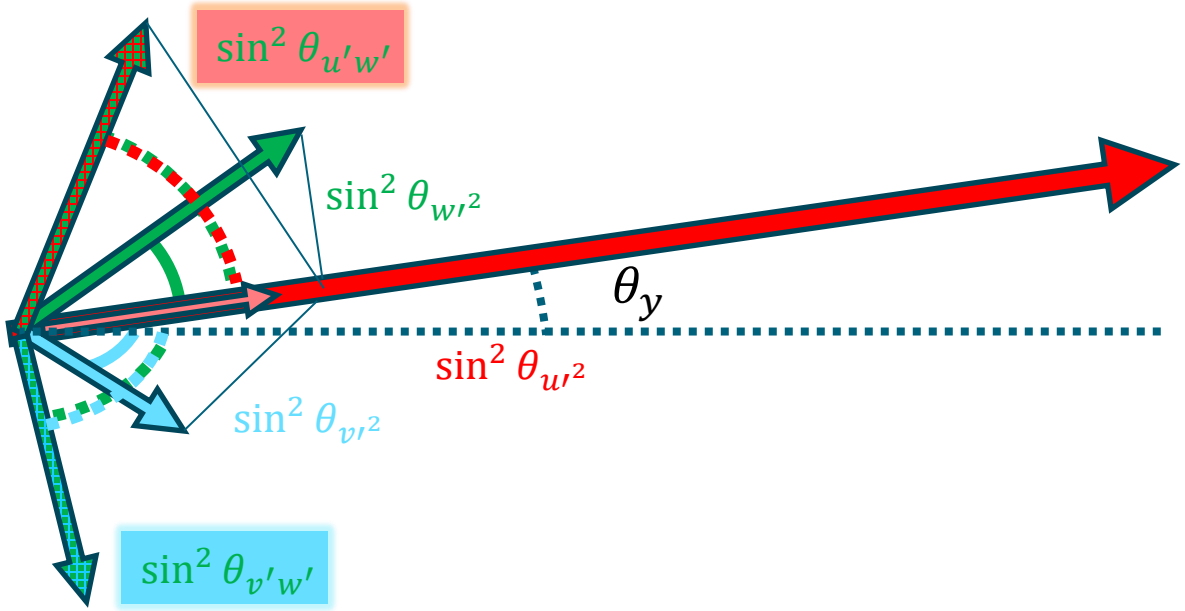

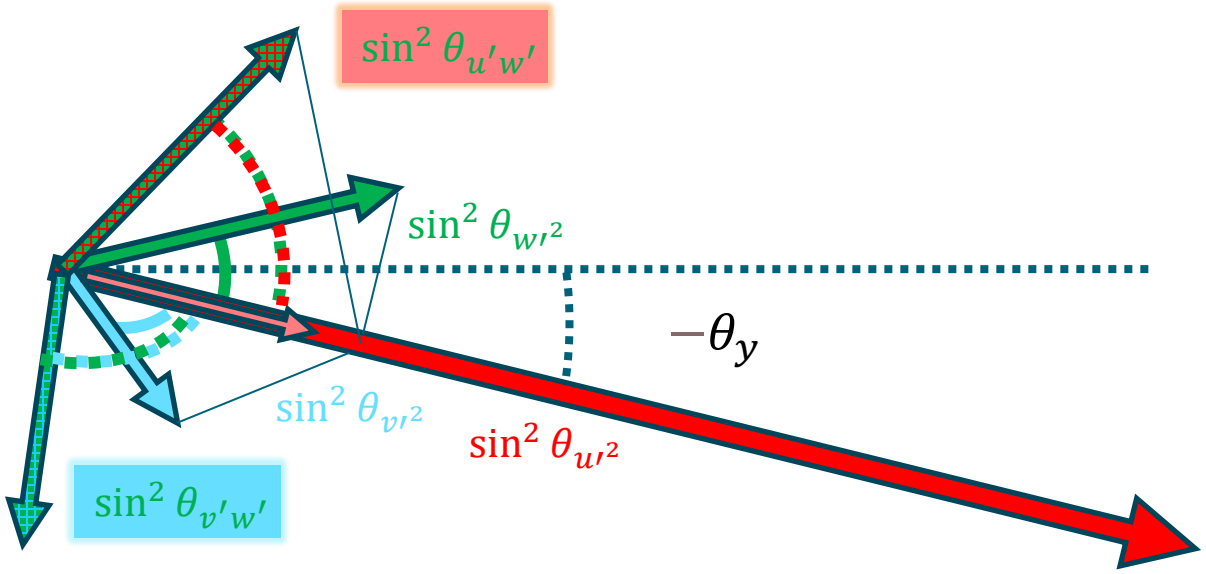

Lidar in Complex Flow for Wind Resource Assessment

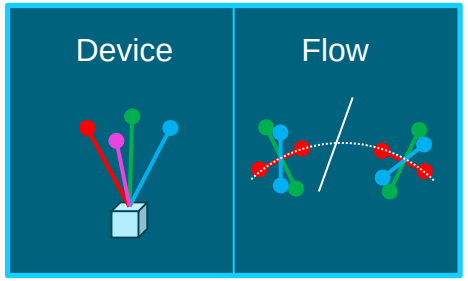

$$\begin{bmatrix} \cos^2\theta_y + \sin^2\theta_y \tan^2\varphi & 0 & \frac{1}{2}\sin 2\theta_y \sec^2\varphi + \tan\varphi \\ 0 & 1 & \tan\varphi \\ \frac{1}{2}\sin 2\theta_y \sec^2\varphi + \tan\varphi & \tan\varphi & \sin^2\theta_y + \sin 2\theta_y \tan\varphi + \left(1+\cos^2\theta_y\right)\tan^2\varphi \end{bmatrix}$$

- Commercially-available RANS-based complex flow correction schemes, as well as those found in the literature, do not include this scalar inflation term
- It shows a relationship between:
  - (1) flow inclination angles, (2) τ_{ij}, and (3) $\sin^2\theta$
- Note that τ_{ij} is generally constrained by the model parametrization
- Lidar in complex flows should exhibit large Scalar-Vector WFR discrepancies

Lidar in Complex Flow for Wind Resource Assessment
Validation Dataset

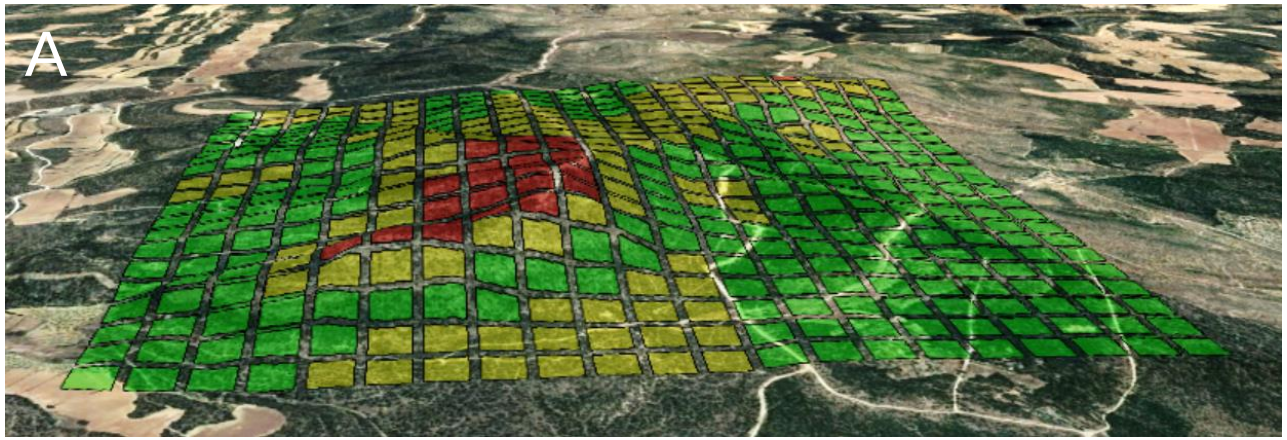

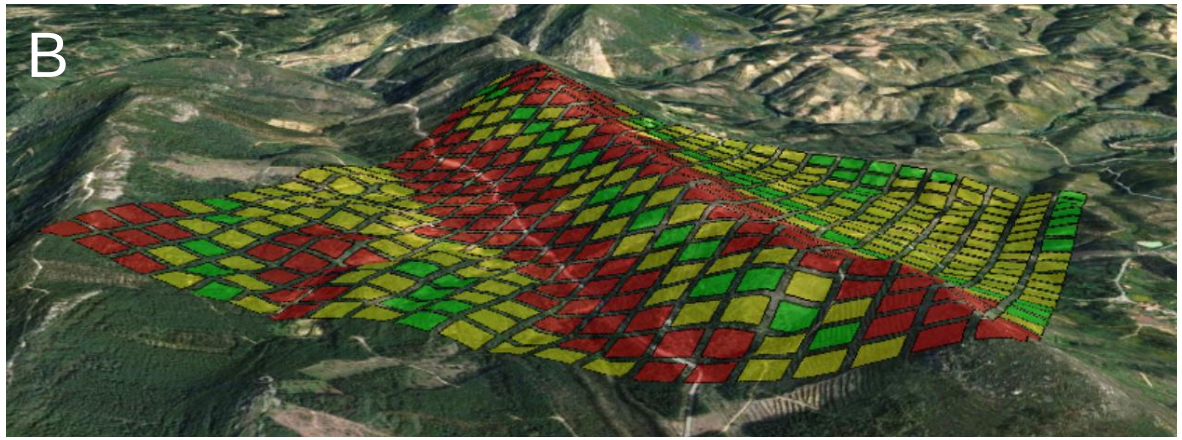

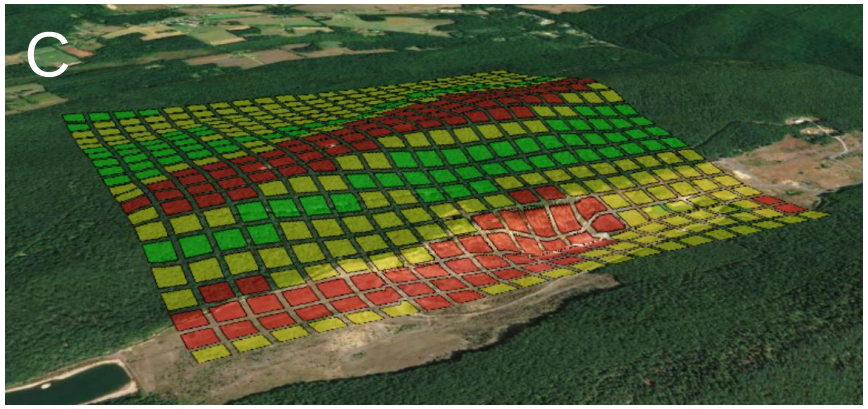

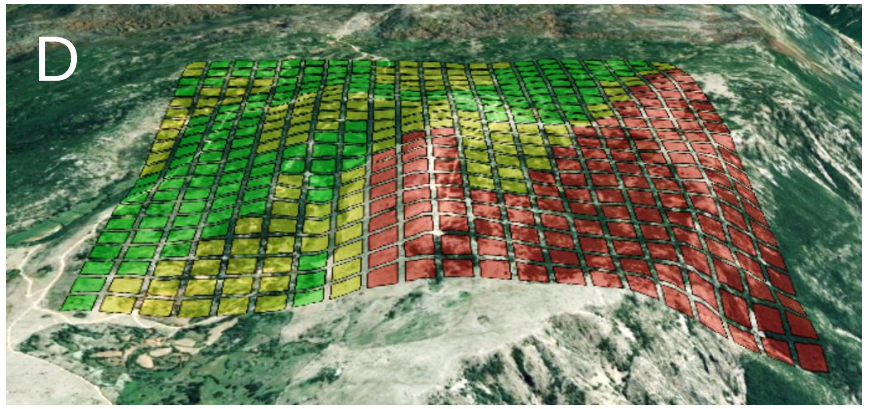

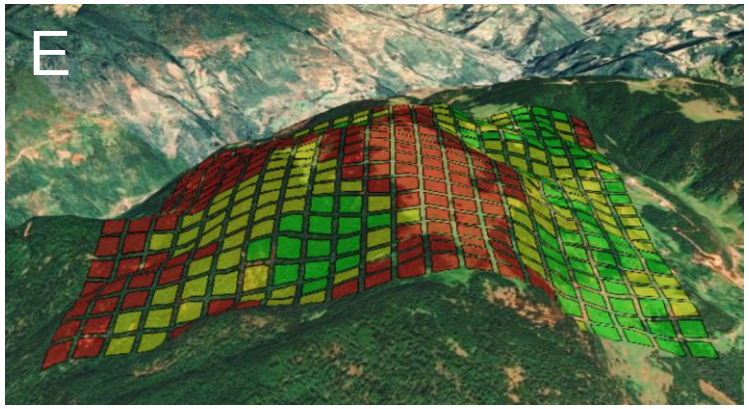

Colors indicate rapid estimate of lidar flow curvature error: <1% 1-3% >3%

Images courtesy of Google Earth and Maxar Technologies

VAISALA

Complex Flow: WindCube v2.0 vs. Anemometry
Lidar Uncorrected

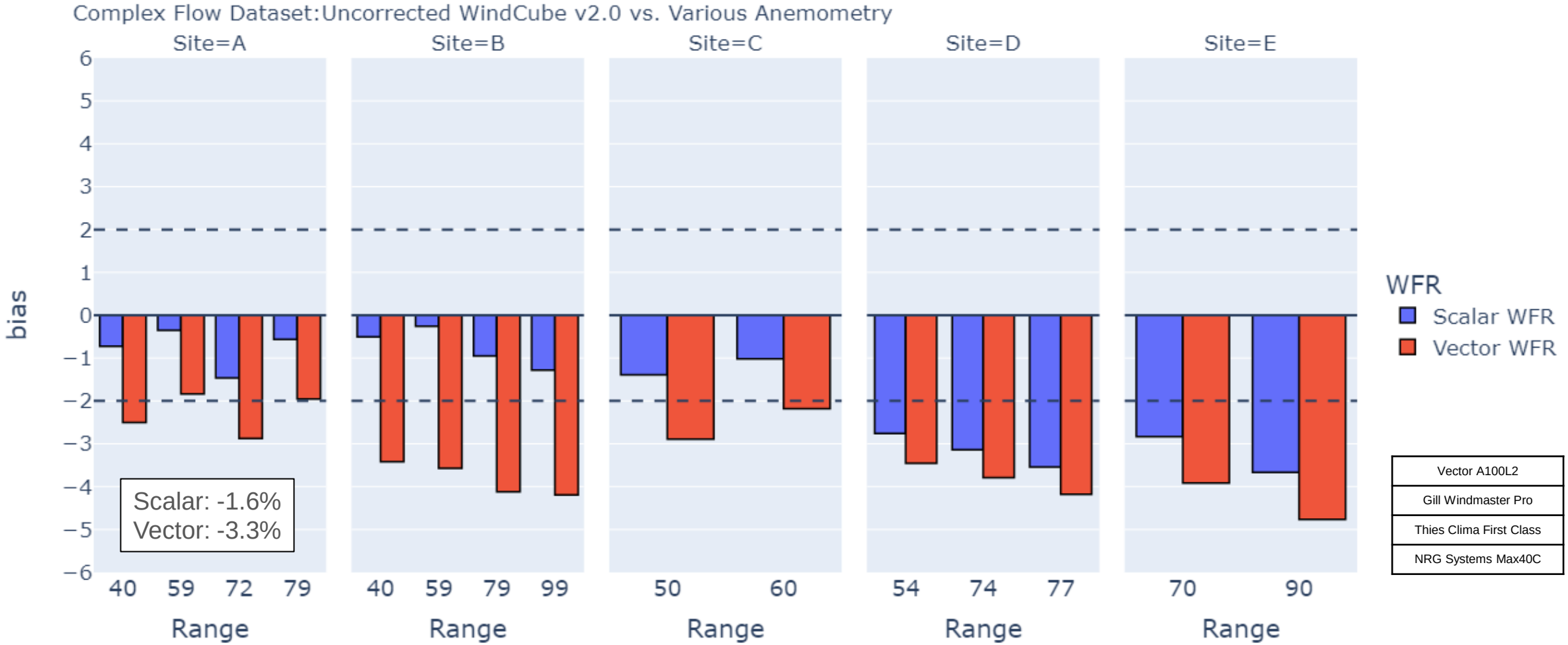

VAISALA

Complex Flow: WindCube v2.0 vs. Anemometry
Lidar RANS-corrected

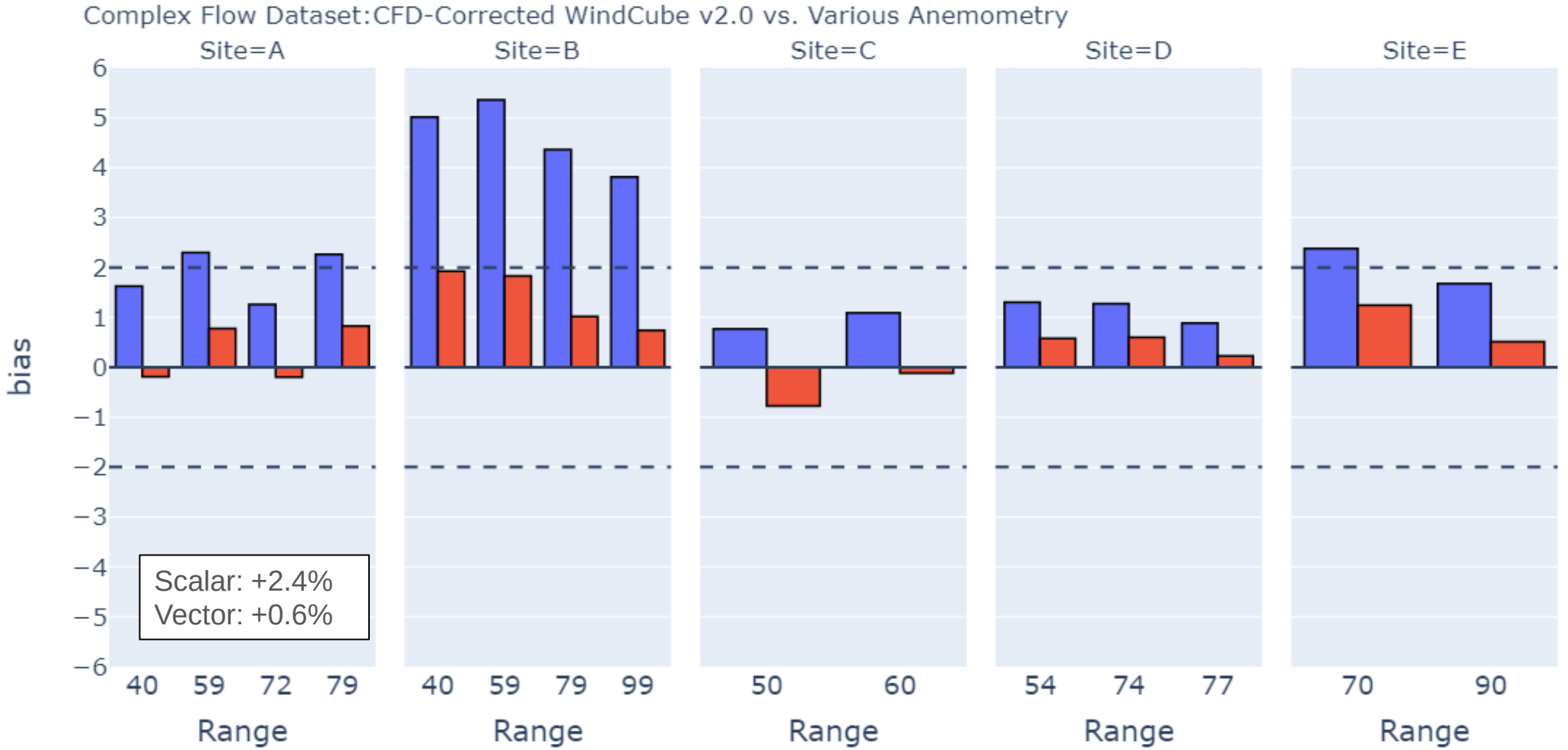

Steady-state RANS
κ-ε closure
Stability modeled via θ and buoyancy
Ekman spiral
Speed-up & angle correction in WFR

WindCube complex flow corrections are available from ArcVera, DNV, DeutscheWindGuard, Fraunhoffer, K2, Meteodyn, Pavana, UL, WindSim

Complex Flow: WindCube v2.0 vs. Anemometry
Lidar RANS-corrected

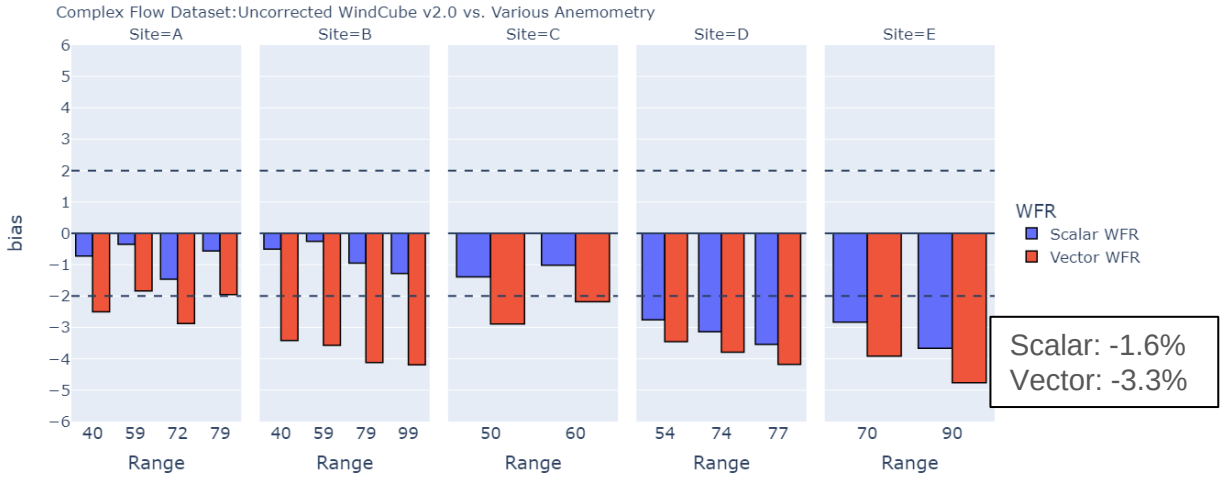

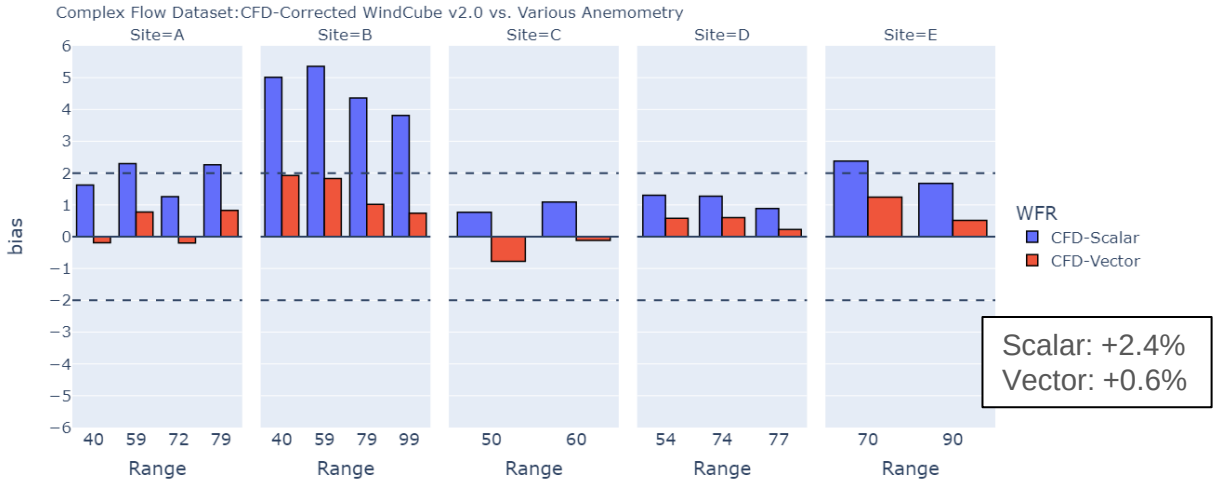

- The Scalar-Vector WFR differences range from +**0.6% to +3.3%**, certainly large enough to influence the performance of RANS-based corrections (which range between **2.0% to 5.4%**)
- In the WindCube v2.1, in flat terrain, Scalar:Vector Hybrid WFR weights are ⅔:⅓ to reduce the scalar inflation term to closely match cup anemometer sensitivities for minimum uncertainties in device Classification
- In complex terrain, the Hybrid WFR weighting can be modified in the WindCube v2.1 firmware to 0:1 to eliminate the scalar inflation term, greatly simplifying the measurement sensitivity and CFD correction.

Point measurement, flat terrain

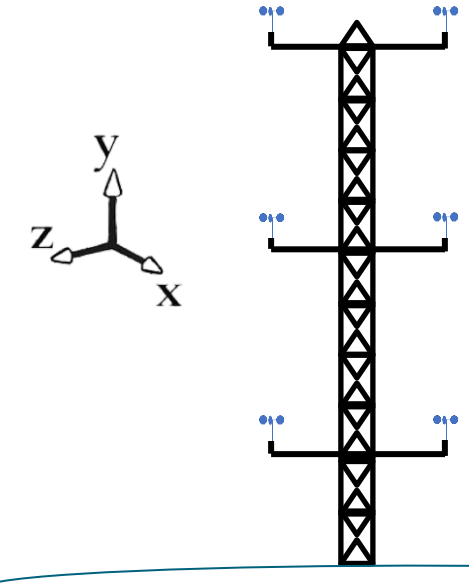

$$\begin{bmatrix} 1 & 0 & 0 \\ 0 & 1 & 0 \\ 0 & 0 & 0 \end{bmatrix} \tau_{ij}$$

Lidar measurement, flat terrain

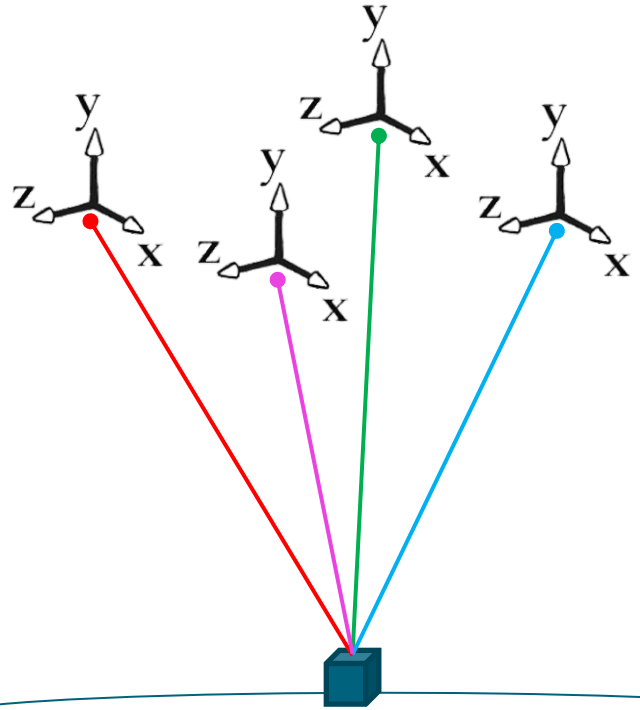

$$\begin{vmatrix} 1 & 0 & \tan\varphi \\ 0 & 1 & \tan\varphi \\ \tan\varphi & \tan\varphi & 2\tan^2\varphi \end{vmatrix} \cdot d\tau_{ij}$$

Point measurement, complex terrain

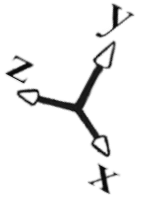

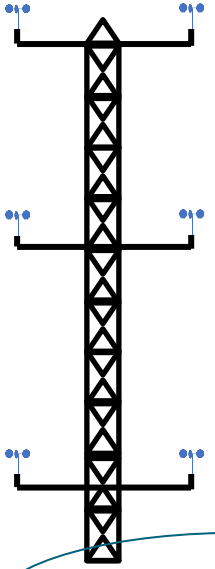

$$\begin{bmatrix} \cos^2\theta_y & 0 & \sin\theta_y\cos\theta_y \\ 0 & 1 & 0 \\ \sin\theta_y\cos\theta_y & 0 & \sin^2\theta_y \end{bmatrix} \tau_{ij}$$

Lidar measurement, complex terrain

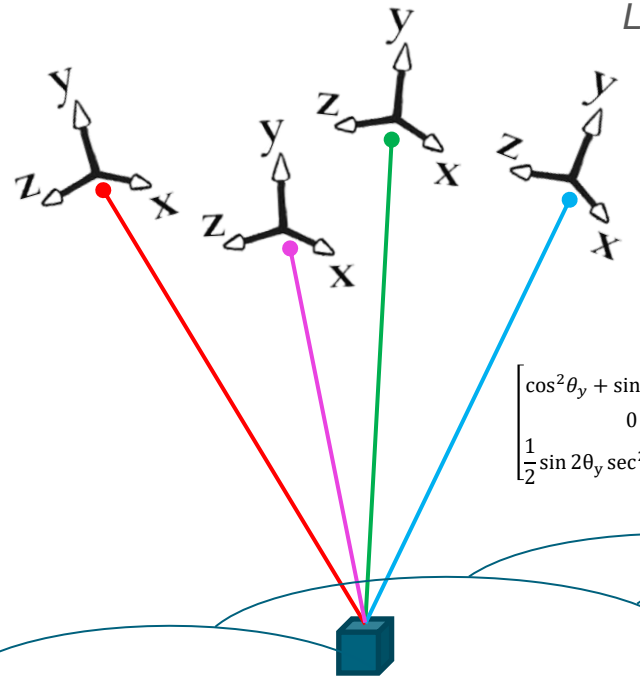

$$\begin{bmatrix} \cos^2\theta_y + \sin^2\theta_y\tan^2\varphi & 0 & \frac{1}{2}\sin 2\theta_y\sec^2\varphi + \tan\varphi \\ 0 & 1 & \tan\varphi \\ \frac{1}{2}\sin 2\theta_y\sec^2\varphi + \tan\varphi & \tan\varphi & \sin^2\theta_y + \sin 2\theta_y\tan\varphi + (1+\cos^2\theta_y)\tan^2\varphi \end{bmatrix}$$

VAISALA

Lidar in Complex Flow for Wind Resource Assessment
Pre-Validation Campaigns and Uncertainty Estimation

- Pre-validation campaigns are carried out in flat terrain using the Classified WFR algorithm, Hybrid WFR with ⅔:⅓ scalar and vector weightings
  - For complex terrain deployments, pre-validation campaigns in flat terrain could be supplemented with an additional analysis for Hybrid WFR weightings near or at 0:1, depending on the complexity of the site.

- Note that in this case, the scalar inflation tensor is present for the anemometry but absent from the lidar.
  - Are we assigning to the lidar uncertainties that, in fact, originate from the cup anemometer?
  - Overestimation of lidar uncertainty due to cup anemometer validations is a concern

Conclusions

- Perturbation method shown to derive scalar sensitivities with good accuracy up to TI = 35%
- Explains physical relationships between Reynolds stress tensor, device geometry, and lateral turbulent fluctuations for cup and ultrasonic anemometers, profiling lidars, and for scalar, vector, and Hybrid WFR
- Application to improve lidar RANS-based complex terrain corrections
- Lidar pre-validations for complex terrain met campaigns should include Hybrid WFR with Vector WFR weighting set at or near 1.0 depending on terrain complexity.

Further Research

- Lidar + LES in complex and simple flow to validate framework in simulated environment
- Precise application to more lidar, anemometer, and CFD measurement campaigns
- Continued research in application to lidar and anemometer 2nd moments

Discussion

- Is this a suitably general to be part of an improved device Classification framework?

$$\bar{U}_{scalar} = U_{vector} + \frac{1}{2U_{vector}} \overline{\left\| \overrightarrow{U'} \right\|_2^2 \sin^2\theta} = U_{vector} + \frac{1}{2U_{vector}} \sum_{i,j=1}^{3} \gamma_{ij} \circ \overline{d\tau_{ij} \sin^2\theta}$$

Thanks for listening!

Contact me at:

andrew.hastingsblack@vaisala.com

VAISALA

References

- Clive, P.J.M: Compensation of Vector and Volume Averaging Bias in Lidar Wind Speed Measurements IOP Conf. Ser.: Earth Environ. Sci. 1 012036, 2008
- Newman, J. F., Klein, P. M., Wharton, S., Sathe, A., Bonin, T. A., Chilson, P. B., and Muschinski, A.: Evaluation of three lidar scanning strategies for turbulence measurements, Atmos. Meas. Tech., 9, 1993–2013, https://doi.org/10.5194/amt-9-1993-2016, 2016.
- Kelberlau, F. and Mann, J.: Better turbulence spectra from velocity–azimuth display scanning wind lidar, Atmos. Meas. Tech., 12, 1871–1888, https://doi.org/10.5194/amt-12-1871-2019, 2019.
- Kelberlau, F. and Mann, J.: Cross-contamination effect on turbulence spectra from Doppler beam swinging wind lidar, Wind Energ. Sci., 5, 519–541, https://doi.org/10.5194/wes-5-519-2020, 2020.
- Sathe, A., Mann, J., Vasiljevic, N., and Lea, G.: A six-beam method to measure turbulence statistics using ground-based wind lidars, Atmos. Meas. Tech., 8, 729–740, https://doi.org/10.5194/amt-8-729-2015, 2015. a, b
- Robey, R. and Lundquist, J. K.: Behavior and mechanisms of Doppler wind lidar error in varying stability regimes, Atmos. Meas. Tech., 15, 4585–4622, https://doi.org/10.5194/amt-15-4585-2022, 2022.
- Rosenbusch, P., Mazoyer, P., Pontreau, P., Allain, P.E., and Cariou, J-P.: Wind speed reconstruction from mono-static wind lidar eliminating the effect of turbulence, Journal of Renewable and Sustainable Energy 13, 063301 (2021)
- Klaas-Witt, T. and Emeis, S.: The five main influencing factors for lidar errors in complex terrain, Wind Energ. Sci., 7, 413–431, https://doi.org/10.5194/wes-7-413-2022, 2022.
- Black, A.: Terrain Complexity Estimation. ACP Resource & Project Assessment, 2023

Appendix: Notes on $d\tau_{ij}$ for profiling lidar

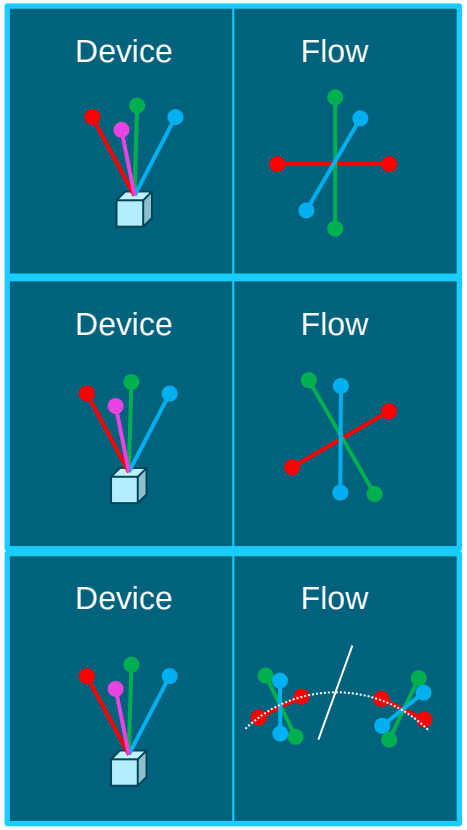

- τ_{ij} replaced by $d\tau_{ij}$
- $u'_N \neq u'_S \Longrightarrow u'_N - u'_S = du'_{N-}$ and $u'_N + u'_S = du'_{N+}$
- Leading weight changes from $^1/_2$ to $^1/_8$ (as $du'_{N-} \neq 2u'_N$)
- $\overline{du'_{N+}{}^2}$, $\overline{du'_{N-}{}^2}$, and $\overline{du'_{N+}du'_{N-}}$ are *slightly* different
- $d\tau_{ij}$ directly integrates Squeeze WFR and convergent lidar geometries to formalism
- $\overline{\sin^2\theta}$ unchanged

Appendix: Notes on $d\tau_{ij}$ for profiling lidar

$$d\tau_{ij} = \begin{vmatrix} +^2 & + - & + - \\ + - & +^2 & + - \\ + - & + - & 2 * -^2 \end{vmatrix} \circ \tau_{ij}$$

- $+^2$: Square of sum of same Reynolds term
  - If beams converge, and are exactly synchronized in time, the turbulence error term is a direct measurement of the Reynolds term
  - If Squeeze WFR applied (wind aligned with beam pair) the error term is a direct measurement of that Reynolds term
  - In cases above, the term carries a factor of exactly 4
  - If beams converge, but are not exactly synchronized in time, this term is reduced depending on the synchronization
  - **If beams diverge and are uncorrelated, term carries a factor of <4**
- $+ -$: Product of one Reynolds sum and one Reynolds difference
  - If beams converge, turbulence error term vanishes (=0)
  - If Squeeze WFR applied (wind aligned with beam pair), turbulence error term vanishes (= 0)
  - **If beams diverge, term carries a factor of ~2 (note sum for symmetric tensor)**
- $-^2$: Sum of squares of differences of Reynolds terms
  - If beams converge, turbulence error term vanishes (= 0)
  - If Squeeze WFR applied (wind aligned with beam pair), turbulence error term vanishes (= 0)
  - **If beams diverge, term carries a factor of ~4**

Abstract

- Wind measurement devices all share a common architecture: measurement geometry of the device probes, and wind field reconstruction algorithms (WFRs) using the measurements. Recent research into 2nd moments (turbulence) using lidars has shown interesting relationships between device geometry and WFR for pulsed and continuous wave (CW) lidars when attempting to measure components of the Reynolds stress tensor (ReST) [REFs, Newman, Sathe, Mann, Kelberlau]. Other research, focused on 1st moments (wind speed) has demonstrated ReST-dependent differences between scalar averaging (reconstruct-then-average) and vector averaging (average-then-reconstruct) [REFs, Lundquist, Rosenbusch]. Both lines of research rely on Reynolds decomposition and by propagation of the mean and turbulent terms through the WFRs.
- In this research, we present a general framework for time-averaged, 1st moment ReST sensitivities in complex, turbulent flows. We demonstrate that scalar averages, widely used in both anemometers and lidars, are invariably modulated by the product of the ReST, the device geometry, and the WFR, a term we call the “scalar inflation tensor”. The derivation expresses the device geometry and fluid orientation as SO(3) rotation groups with identical axes, followed by Reynolds decomposition, time-averaging, and both 1st and 2nd order binomial approximations of the WFR. This allows expression of the scalar inflation tensor compactly for various measurement geometries.
- In simple flows, the scalar inflation tensor is small and can often be neglected. However, in non-homogeneous flows, such as unstable conditions or complex flows, lidar and anemometer scalar averages have non-negligible ReST sensitivities on the order of a few percent. In complex flows, the scalar inflation tensor is the same order of magnitude as flow-induced biases and can easily confound CFD- or LES-based correction schemes. [REFs, IEA, Klaas-Witt]. Hybrid and vector averaging schemes are shown to systematically improve correlations between CFD-corrected lidars and collocated met masts. These improvements to measurement accuracy in complex terrain could be used to refine site calibration, wind resource assessment, power curve measurements, and power performance testing.
- There is not a comparable vector inflation tensor error term. Wind energy literature often describes vector averages as exhibiting low biases compared to simultaneous scalar averages. However, the ubiquity and complexity of the scalar inflation tensor implies that this is inverted: we should instead be describing scalar averaging biases and taking care to mitigate them in our measurement campaigns.